

# Mechanical Characterization of Al-Cu Materials Fabricated by Powder Metallurgy under Quasi-static and Dynamic Compressive Loadings

Tatiana Simeonova<sup>1,\*</sup>, Rumen Krastev<sup>1</sup>, Georgi Stoilov<sup>1</sup>, Vasil Kavardzhikov<sup>1</sup>

Institute of Mechanics at Bulgarian Academy of Sciences, Bulgaria<sup>1</sup>  
tsimeonova@imbm.bas.bg

**Abstract:** This study investigates the mechanical behaviour of Al10Cu materials fabricated through powder metallurgy and subjected to quasi-static and dynamic compressive loadings. The materials were sintered and tested under controlled conditions to evaluate their compressive strength. Quasi-static tests were performed at a constant strain rate of  $0.003 \text{ s}^{-1}$ , while dynamic tests were conducted at strain rates corresponding to impact speeds of about 10 m/s and 20 m/s. The results indicate that sintered Al10Cu materials are suitable for applications under high-strain impact loadings due to their high energy absorption. These findings highlight the potential of powder-metallurgy-derived Al10Cu alloys for applications requiring high strain rate performance, offering insight into their suitability for use in dynamic environments.

**Keywords:** Al10Cu MATERIALS, POWDER METALLURGY, COMPRESSIVE STRENGTH, HIGH STRAIN RATE PERFORMANCE

## 1. Introduction

Investigations of light metal matrix materials and composites produced under solid-state conditions have gained great attention in the last decade. The general reason that led the researchers in this direction is that solid-state processing employs lower processing temperatures [1,4] and thus gets closer to the EU's sustainable consumption and production policies. Generally, Aluminium and its alloy are widely used as a base for the production of metal matrix composites (MMC), reinforced by ceramic particles (SiC, B<sub>4</sub>C, Al<sub>2</sub>O<sub>3</sub>, TiC and WC), because of their advanced properties like reduced weight, high specific stiffness, excellent strength/weight ratio, increased mechanical and thermal performance, improved strength, higher elastic modulus, and superior wear resistance compared to unreinforced matrices [1,2,4,7,12]. For the production of MMC with such enhanced properties a range of investigations are done concerning the quality of the matrix material, the type, size and quantity of the reinforcing particles, the influence of production process parameters on the structure and properties of the developed materials, and so on. And the first step is always choosing the best matrix material. The primary alloying elements in aluminium powder are copper, magnesium, and zinc [4], with copper being the most significant due to its ability to enable additional age hardening in Al-Cu alloys. In the Al-Cu sintering process, a eutectic liquid forms at 548°C along the Al-Al<sub>2</sub>Cu boundaries [5]. This liquid phase enhances diffusion between the powders by penetrating grain boundaries during sintering [6]. From the literature review, it has been proved that Al-Cu matrices possess great potential for developing MMCs with improved properties via solid-state fabrication techniques such as powder metallurgy and are commonly used for the production of lightweight functional components. Different matrix content had been investigated as Al-4 wt% Cu [1,2,4,9], Al-3%Cu [3,10,13,19], Al-6%Cu [3,13,19], Al-4.5 wt.% Cu [8] and Al-9 wt.% Cu [13]. It is observed that the addition of copper to the aluminium matrix allows for a higher densification of the materials [4,19], which gets us to the point of this investigation aiming to investigate the properties of Al-10wt%Cu produced by the conventional PM technique. Some investigations are already made by increasing the amount of Cu till 9 vol.% for production of Al-Cu composite by vacuum and microwave sintering techniques [13] and an increase in steps of 5 wt% (5%, 10%, 15%, and 20%) for developing in-situ Al-Cu metal matrix composites using microwave sintering and friction stir processing [14] which revealed that the addition of copper enhanced the mechanical and electrical properties of the MMC up to 10wt%Cu and beyond which it decreased. The mechanical properties are accessed through compression testing particularly under dynamic conditions, due to the lack of sufficient data for the response of Al-Cu materials, produced by the PM technique, to high strain rates of deformation [15].

This study aims to comprehensively evaluate the mechanical behaviour of Al10Cu alloys fabricated through powder metallurgy under varying compressive loading conditions. Specifically, the

research seeks to assess the compressive strength and energy absorption capabilities of sintered Al10Cu materials by subjecting them to quasi-static and dynamic compressive tests. By systematically analysing the performance of Al10Cu alloys under these distinct loading regimes, the study aims to determine their suitability for applications that require robust energy absorption and high strain rate performance.

## 2. Materials and methods

Aluminium-based Al-10 wt.% Cu alloy was fabricated using aluminium powder and copper powder as the primary materials. The Al powder employed had a particle size of  $\leq 325$  mesh, while the Cu powder also possessed a particle size of  $\leq 325$  mesh. To create the Al-10 wt.% Cu base alloy, the Al and Cu powders were first mixed in the desired proportions. The combined powders were then subjected to ball milling with a ball-to-powder ratio of 6:1. This milling process was carried out for 5 hours at a rotation speed of 500 rpm using a high-energy ball mill, ensuring a uniform distribution of Cu particles within the Al matrix. Following ball milling, the powder mixtures were compacted using a hydraulic press. Compaction was performed in a cylindrical steel die with a diameter of 16 mm at a pressure of 160 MPa, resulting in the formation of green bodies. These green bodies were subsequently sintered in a controlled atmosphere furnace under argon (Ar) to prevent oxidation and contamination. The sintering process was conducted at a temperature of 530°C for 3 hours. After sintering, the samples were allowed to cool slowly within the furnace to ensure uniform microstructural development and to minimize thermal stresses. The powder metallurgy technique utilized for the production of the Al10Cu alloy is illustrated in Fig. 1.

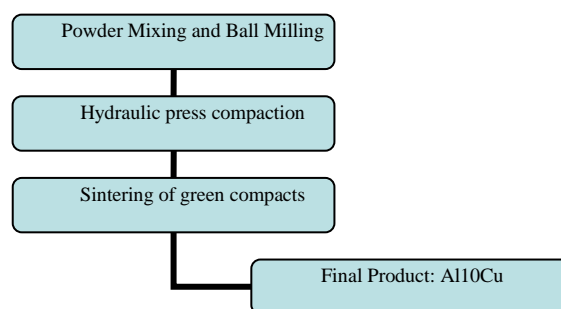


Fig. 1 Production process chart

The sintering process influences the material's microstructure and properties [6]. The specimens used to determine the mechanical properties of the fabricated materials are cylindrical with a diameter of 10 mm and height of 15 mm (for quasi-static testing) and a diameter of 5 mm and height of 5 mm (for dynamic testing). The quasi-static compression tests were conducted on a Zwick Roell HA250 servo-hydraulic testing machine at a constant low strain rate of  $0.003 \text{ s}^{-1}$ . The dynamic compression tests by the Split Hopkinson Pressure Bar (SHPB) apparatus were carried out at high

strain rates of about  $\sim 1500 \text{ s}^{-1}$  and  $\sim 3200 \text{ s}^{-1}$ , corresponding to impact speeds of about 10 m/s and 20 m/s. A modified version of the Split Hopkinson-Kolsky Pressure Bar is used, specially designed for impact testing of porous and light materials, which includes an aluminium alloy incident bar and transmitted bar in the form of a steel tube. To access high strain rates compression properties of the tested materials the incident bar is stroked and a compressive pulse is generated which propagates through the incident bar. Part of the incident pulse signal is reflected as the reflected pulse into the incident bar at the incident bar/specimen interface. The remainder passes through the sample, deforming it plastically and continuing forward into the transmitted bar as the transmitted pulse [15]. The transmitted pulse is compressive, and its instantaneous amplitude is related to the instantaneous stress in the specimen. The stress information can be obtained as a parametric function of time. The instantaneous strain was obtained by integrating the incident and the transmitted pulse upon time. The modified version of the SHPB and the corresponding mathematical apparatus for calculating the strain are described in [22].

### 3. Results and discussion

The analysis of the compression test results is based on structural changes that occur during the PM production process of Al-Cu alloys. It is known, according to the Al-Cu phase diagram, that five intermetallic phases of  $\text{Al}_2\text{Cu}$ ,  $\text{AlCu}$ ,  $\text{Al}_3\text{Cu}_4$ ,  $\text{Al}_2\text{Cu}_3$ , and  $\text{Al}_4\text{Cu}_9$  could be formed in the Al-Cu system through solid-state phase transformation [10,11,18] and among these  $\text{AlCu}$ ,  $\text{Al}_2\text{Cu}$ , and  $\text{Al}_4\text{Cu}_9$  are the stable phases [14]. Thermodynamically  $\text{Al}_2\text{Cu}$  and  $\text{Al}_4\text{Cu}_9$  phases evolve first due to their lowest formation energy [11,18] and the remaining intermetallic phases are formed after them depending on temperature and time.  $\text{Al}_4\text{Cu}_9$  is a brittle intermetallic phase and its formation is desirable to be avoided [14].  $\text{Al}_2\text{Cu}$  is more stable and the long thermal processing time is sufficient to convert  $\text{AlCu}$  to  $\text{Al}_2\text{Cu}$ , which can explain the fact that increasing Cu content only results in the formation of  $\text{Al}_2\text{Cu}$  in the fabricated composites [10]. When sintering the Al-Cu system at temperatures exceeding the solidus, a liquid phase forms, which migrates along particle boundaries, fills pores and infiltrates aluminium grain boundaries. Upon slow cooling after sintering, this phase precipitates at the grain boundaries as  $\text{Al}_2\text{Cu}$  [4]. Therefore, the microstructure of the Al10Cu matrix material is expected to consist of aluminium grains with dissolved copper surrounded by coarse copper precipitated in the form of the  $\text{Al}_2\text{Cu}$  phase at the grain boundaries of aluminium grains [1, 4]. The precipitate morphology shows a combination of linear structures at grain boundaries and dot-like features within the grains [4]. The  $\text{Al}_2\text{Cu}$  phase is believed to be the main reason for the enhanced mechanical properties of the tested Al10Cu alloys, summarised in Table 1.

**Table 1:** Average values of the mechanical properties of tested materials.

Specimen	quasi-static compression	high impact dynamic compression	
		5x5	5x5
Dimensions [mm]	10x15	5x5	5x5
strain rate [ $\text{s}^{-1}$ ]	0.003	1500-1900	3200
Modulus of elasticity [GPa]	10.4	7.8	5.62
YS(offset=0.2%) [MPa]	64.4	79	74
Compressive strength [MPa]	431	418	1445
Deformation $\varepsilon$ [%]	60	44.6	79.1

Quasi-static compression test results are presented in Fig. 1 with the stress-strain curves of 6 tested powder-metallurgy-derived Al10Cu specimens. It can be observed that the stress-strain curves of the specimens under quasi-static compression are very similar. All samples go through the stages of elastic compression of the compact up to about the proportional limit and yielding, strain hardening with particle inelastic deformation under normal and shear forces, and non-uniform deformation at compressive strength with two conic shear bands begin to develop along the diagonal axes of the compact, at  $45^\circ$  to the loading direction [20,21].

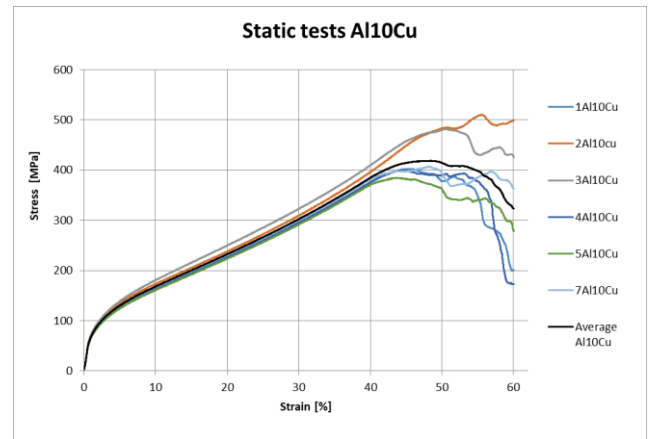


**Fig. 1** Quasi-static tests result at a constant strain rate of 0.003/s

Deformation concentrated within shear bands leads to a decrease in the load-bearing capacity of the compact, culminating in complete failure as bonded particles separate along the shear bands, initiating from the corners of the cylindrical compact specimen [21]. The stress-strain curves are smooth up to 40% deformation in all tested specimens. The observations reveal that the yield stress in all the specimens is almost equal and the material continues to strain harden even after 30% plastic strain. The differences in quasi-static compression response are notable after 40% deformation, which is believed to be due to different amounts of pores and microcracks, formed at the grain boundaries during the production of PM alloys based on Al and Cu powders [1,4,8], even after the sintering process [19]. The pores primarily formed in the matrix, while the microcracks predominantly appeared at the joint between the matrix and Cu particles [20]. These defects act as stress risers causing components to fracture and deform more easily [19]. The actual crushing of different specimens is presented in Table 2.

**Table 2:** Actual crushing characteristics at different strains

$\varepsilon, \%$	10%	20%	30%	40%	50%	60%
1						
2						
3						
4						
5						
7						

All specimens showed almost the same degrees of barrel-shaped deformation as the strain increased, although more serious failure behaviours were not observed. The first formation of the shear cracks is visible by the naked eye after 40 % deformation and the exact values for every specimen are shown in Table 3. At 50% deformation, all specimens possess severe failure cracks.

The results from dynamic compression tests are shown in Fig. 2 for moderate strain rates of 1500/s and Fig. 3 for high strain rates of 3200/s and the tested specimens are presented in Table 4. Figure 2 shows the results of dynamic tests at moderate strain rates of 1500/s. The resulting curves are not as smooth as the ones under quasi-static loading conditions.

**Table 3: The formation of the visible shear cracks**

Specimen	Deformation $\epsilon, \%$	Picture
1Al10Cu	42	
2Al10Cu	47	
3Al10Cu	43	
4Al10Cu	41	
5Al10Cu	40	
7Al10Cu	41	



**Fig. 2 SHPB dynamic test results at 10-12 m/s**

There is some gradual strain hardening up to 5% strain in the specimen tested at 1500/s strain rate after which the flow stress drops. The same fluctuations during the strain hardening are observed in the interval between 30 and 40% deformation. The stress-strain curves under dynamic compression reveal the same failure mode at different strain rates. The ultimate strength and failure strain increased with the strain rate. The three types of failure could be observed in specimens under different impact velocities: plastic failure, splitting failure and smash failure [20]. Fig. 3 shows the results of dynamic tests done at higher strain rates of 3200/s which reveal similar to quasi-static curves trends.

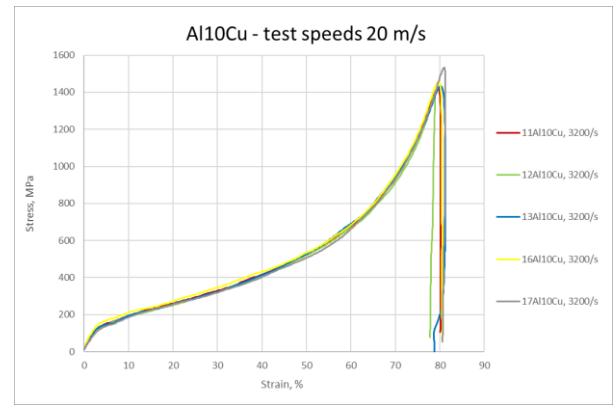


**Fig. 3 SHPB dynamic test results at 20m/s**

In our case, all tested at 1500/s specimens exhibited plastic failure, while at some tested at 3200/s partial splitting was observed. The plastic failure occurred at impact velocities greater than 9 m/s while smash failure occurred at impact velocities over 19 m/s. The elastic stage is distinct in all tested specimens and the hardened state lasts continuously under dynamic compression. By comparing the stress-strain relationship it was found that the dynamic mechanical properties at strain rates of 3200/s were better than those at 1500/s, but the kinetic energy required to produce the same failure stage is the same. The comparison of the specimens at different strain rates showed that the compression strength of the material increases with the strain rate, but the variation in yield strength is negligible.

**Table 4: The formation of the visible shear cracks**

Before	After	Before	After	Before	After
8Al10Cu – 1500/s		9Al10Cu – 1500/s		10Al10Cu – 1500/s	
15Al10Cu – 1900/s		11Al10Cu – 3200/s		12Al10Cu – 3200/s	
13Al10Cu – 3200/s		16Al10Cu – 3200/s		17Al10Cu – 3200/s	

A comparison of all tested samples at all tested strain rates is shown in Fig. 4. The compressive strength increases from about 400 MPa at quasi-static rates (0.003/s) to 1400 MPa at high strain rates (3200/s) and the strain corresponding to the maximum compressive stress is shifted from about 40% to 80%. The specimens displayed very little change during the elastic stage. It was also found that the change in strain rate had little effect on the elastic modulus which lowers with the rise of the strain rate (table 1). The elastic modulus obtained under quasi-static loadings is approximately 10 GPa, about 50% higher than that obtained at strain rates of 3200/s (5 GPa). The yield strength at high strain rates is higher than that under quasi-static loadings. Generally, yield and ultimate strengths increased with strain rate, while the lower failure strain is observed at a strain rate of 1500/s. As mentioned before, the slight differences in properties could be due to the different densification of specimens [20], although this is not obvious from compression tests.

The difference between the quasi-static and moderate and high-strain dynamic tests is that the stress-strain curves reached higher stresses at high strain rates. The higher strain hardening at higher strain rates is also notable, which is typical of fcc metals and is due to the suppression of dynamic recovery mechanisms at high strain rates [15]. The same trend of all the curves at all tested speeds leads to the conclusion of similarity in the intermetallic content of all of the specimens and based on previous research of the microstructural evolution of Al-Cu materials fabricated through powder metallurgy

it is expected that Cu atoms diffuse into the Al matrix during the synthesis of Al-Cu alloy and Al<sub>2</sub>Cu precipitates in a solid solution of Al(Cu). That is why we believe that observed mechanical properties are governed by indirect strengthening of the Al matrix which is expected to be due to Al(Cu) solid solution strengthening and the structural Al<sub>2</sub>Cu precipitate strengthening [16]. Precipitation hardening of aluminium alloys can involve either precipitate shearing for coherent precipitates, or precipitate by-passing by the dislocations [16]. To be positive about the type of precipitation hardening mechanisms - precipitate shearing or precipitate by-passing, additional analysis and TEM observations must be done involving the determination of the precipitate radius.

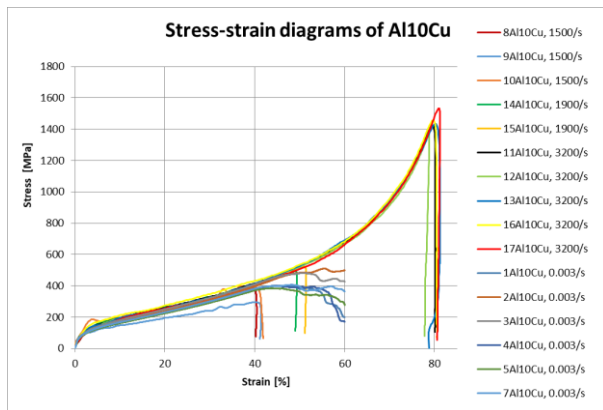


Fig. 4 Comparison of all tested samples at all tested strain rates

Generally, the advanced compressive properties of Al-Cu alloys are led by three possible strengthening mechanisms including the Orowan strengthening mechanism of uniform distribution of Cu particles, enhanced dislocation density due to the large mismatch between the thermal expansion coefficient of copper particles and the aluminium matrix and the dispersion hardening effect of the hard Cu particles into the soft Al matrix [13]. However, the strength of the composites does not depend on a unique mechanism and several mechanisms may act simultaneously. The dislocations could be piled up against the grain boundaries turning them into a barrier to dislocation motion and thus increasing the strength of the alloy [17]. The precipitates could also act as a barrier to the dislocation movement, requiring greater stress to move the dislocations [17]. Also, precipitates along the grain boundaries act as a pinning agent for the grain boundary sliding. That is why the distribution of the secondary phase precipitates within the grains and along the grain boundaries is responsible for increasing the compression strength [17].

The deformation mechanism of the tested compacts includes particle separation occurring primarily at the interparticle bond region with ductile fracture type of the interparticle bond while originally non-contacting particles are developing contacts with neighbouring particles during deformation and as a result of particle inelastic deformation the contact area between bonded particles increases over the interparticle bond area. During the non-uniform deformation in the samples voids and macrocracks were observed in the interparticle bond region. The growth and coalescence of these voids eventually led to the development of macrocracks and complete separation of the interparticle bond region [21].

#### 4. Conclusions

The current investigation focuses on Al-Cu matrices material with enhanced mechanical properties under compression loadings, which will be incorporated with different ceramic particles in our future work. The major conclusions that could be drawn back are:

1. Aluminium-based Al-10 wt.% Cu alloy was successfully fabricated through the powder metallurgy method
2. The increased compressive strength up to 1445 MPa and deformation up to 80% at high strain rates (3200/s) were experimentally proved by SHPB testing.

3. The significant improvement in mechanical properties is attributed to the dispersion hardening effect of hard Cu particles in the soft Al matrix.

#### 5. Acknowledgments

The research was supported by the European Regional Development Fund within the OP Science and Education for Smart Growth 2014–2020, Project CoE “National Center of Mechatronics and Clean Technologies”, BG05M2OP001-1.001-0008.

#### 6. Funding

This research was funded by the Bulgarian National Science Fund, Project **KII-06-H77/5** "Self-lubricating hybrid aluminum metal matrix composites: synthesis, experimental and computer modeling of mechanical and tribological properties".

#### 7. References

1. A. Wąsik, B. Leszczyńska- Madej, P. Noga. The Int. J. of Adv. Man. Tech (2024) **134**:3611–3620
2. S. Jain, R.S Rana, P. Jain. Int. Res. J. of Eng. and Tech (2016), Vol: 03, Issue: 01
3. M.N. Khan, S. Narayan, A. Rajeshkannan A.K. Jeevanantham. Materials Today: Proceedings **22** (2020) 2499–2508
4. A. Wasik, B. Leszczynska-Madej, M.Madej, M. Goły. Materials (2023) **16**, 5492.
5. G.B. Schaffer, T.B. Sercombe, R.N. Lumley. Mater. Chem. Phys. (2001) **67**, 85–91.
6. K. Sang-Chul, K. Moon-Tae, L. Sungkyu, C, Hyungsik, A. Jae-Hwan. J. Mater. Sci. (2005) **40**, 441–447.
7. P. R. Matli, R. A. Shakoor, A. M. A. Mohamed, M. Gupta. Metals (2016) **6**, 143
8. K.N. Manjunath, G.B. Krishnappa. Materials Today: Proc. **5** (2018) 3019–3026
9. R. S. Bonatti, A. D. Bortolozzo, R. F. G. Baldo, E. Poloni, W. R. Osório. Metals (2023) **13**, 1710
10. S. LUO, Y. WU, B. CHEN, M. SONG, J. YI, B. GUO, Q. WANG, Y. YANG, W. LI. Z. YU. Trans. Nonferrous Met. Soc. China **32**(2022) 3860–3872
11. R. Ali, F. Ali, A. Zahoor, R. N. Shahida, N. H. Tariq, T. He, M. Shahzad, Z. Asghar, A. Shah, A. Mahmood, H. B. Awais. J. of Alloys and Comp. **889** (2021) 161531
12. O. Emadinia, M. T. Vieira, M. F. Vieira. Met. **2020**, 10, 1416
13. P. R. Matli, U. Fareeha, R. A. Shakoor, A. M. A. Mohamed. J. Mater Res. Technol. (2018) **7**(2):165–172.
14. R. Malik, P. A. Bajakke, K. K. Saxena, A. Lakshmikanthan, A. S. Deshpande, S. Mabuwa, V. Masomi. Mater. Res. Express **9** (2022) 066507
15. K. S.M. Sonti, B. Dash, K.V. Vamsi, H. Bandyopadhyay, B. Ravisankar, K. Sivaprasad, S. Karthikeyan. J. of All. and Comp. **873** (2021) 159767
16. A. Joseph, V. Gauthier-Brunet, A. Joulain, J. Bonneville, S. Dubois, J-P. Monchoux, F. Pailloux. Mat. Char. **145** (2018) 644–652
17. H.K. C. Mohan, S. Devaraj, K.S. N. Swamy. J. of Mat. Eng. and Perf. (2021) **30**:2433–2438
18. D. Kim, K. Kim, H. Kwon. Materials (2021), **14**, 266.
19. M. N. Khan, S. Narayan, A. Rajeshkannan. AIMS Mat. Sci. (2019) **6**(3): 441–453.
20. X. Tang, Z. Wang, J. Yin, J. Yi. Adv. in Mat. Sci. and Eng. 2021, Article ID 5518172, 9 pages
21. M. Guden, T. E. Celik, E. Akar, S. Cetiner. Materials Characterization **54** (2005) 399–408
22. R. Krastev, V. Kavardzhikov, T. Simeonova. Math. Modeling (2024), Vol. 8 (to be published)